J Nanopart Res (2015) 17:407
DOI 10.1007/s11051-015-3195-y

RESEARCH PAPER

Antibacterial performance of nano polypropylene filter media containing nano-TiO_2 and clay particles

Sara Shafiee · Mohammad Zarrebini · Elham Naghashzargar · Dariush Semnani

Received: 22 May 2015 / Accepted: 23 September 2015 / Published online: 16 October 2015

Abstract Disinfection and elimination of pathogenic microorganisms from liquid can be achieved by filtration process using antibacterial filter media. The advent of nanotechnology has facilitated the introduction of membranes consisting of nano-fiber in filtration operations. The melt electro-spun fibers due to their extremely small diameters are used in the production of this particular filtration medium. In this work, antibacterial polypropylene filter medium containing clay particles and nano-TiO_2 were made using melt electro-spun technology. Antibacterial performance of polypropylene nano-filters was evaluated using *E. coli* bacteria. Additionally, filtration efficiency of the samples in terms fiber diameter, filter porosity, and fiber distribution using image processing technique was determined. Air permeability and dust aerosol tests were conducted to establish the suitability of the samples as a filter medium. It was concluded that as far as antibacterial property is concerned, nano-fibers filter media containing clay particles are preferential to similar media containing TiO_2 nanoparticles.

S. Shafiee · M. Zarrebini · E. Naghashzargar · D. Semnani (✉)
Department of Textile Engineering, Isfahan University of Technology, Isfahan 84156-83111, Iran
e-mail: d_semnani@cc.iut.ac.ir

E. Naghashzargar
e-mail: e.naghashzargar@tx.iut.ac.ir

Keywords Nano-fibers · Antibacterial · Melt electro-spun · Membrane · Image processing · Polypropylene · Clay particles

Introduction

Separation of hazardous pathogenic microorganisms in wet filtration operation using antibacterial filter medium has been a challenge for decades. Mirjalili et al. attempted to impart antibacterial ability to cellulose fabric using nano-silver solution treatment at various concentrations (Mirjalili et al. 2013). Research on water decontamination using filter media coated with 6–12-nm silver nanoparticles has also been reported. Results confirmed that higher concentration of silver solutions and exposure time yield better bacterial separation (Phong et al. 2009). Polanco studied the toxicity of bacteria membrane of selected antibacterial peptides containing 10–45 positively charged amino acids (Polanco 2013). Coaxial electro-spinning technology was used to fabricate core–sheath antibacterial nano-fibers by blending active agents such as silver and metal oxide nanoparticles (Gao et al. 2014).

Polymer–particle composites due to their diverse mechanical and morphological properties have attracted attention of material scientists. Generally, polymers are blended with mineral fillers or particles for various applications (Akinci 2009). In this work,

antibacterial performance of nano-fibers polypropylene and nano-TiO_2 particles incorporating clay fillers (nPP) has been evaluated.

Polypropylene is universally regarded as the preferred thermoplastic material due to combination of performance and price (Housmans et al. 2009). Three main types of polypropylene including isotactic, atactic, and syndiotactic are available (Zhong et al. 2014). Electro-spun nano-fibers are employed in various applications such as filtration media due to their high specific surface area which positively affect media porosity and tortuosity (Ghiasi et al. 2014). Electro-spinning process is capable of producing fibers with diameters ranging from nano- to micro-scales. Electro-spun fibers are generally produced from polymer solution. However, certain polymers such as polyolefin cannot be dissolved by common solvents. Thus polypropylene fibers are produced via melt-blown or melt extrusion method (Fang et al. 2012). Among various parameters, molecular weight is the most influential factor that affects fiber diameter (Lyons et al. 2004).

Fillers such as clay are extensively used in various applications ranging from industrial to hygienic consumable and health care. Recently, the use of clays as additives or fillers with the aim of gaining desirable effects in polymers has attracted the interest of researchers (Uddin 2008). Alumina and silica, as the two principle constituents of clay, easily form most of earth crust. Chemical analysis of clay points to the fact that clay is largely composed of alumina and silica and partly small quantities of calcium, iron, magnesium oxide, and other elements (Nayak et al. 2007). Clay-based materials are well known both as traditional and novel functional nano-scale functional composite components. Advanced clay-based materials have been extensively used in various industries ranging from paper and pharmaceuticals to catalysts or catalyst supports (Bhorodwaj et al. 2011). Clays exhibits high cation exchange capacity, high specific surface area, and colloid properties with affinity to absorb both organic and inorganic substances (Parolo et al. 2011). High surface area and high cation exchange capacities enable clay to free metals from inorganic contaminants (Gitipour et al. 2006). Antibacterial performance of cotton fibers treated with montmorillonite and modified clays is superior to cotton fibers treated with ammonium quaternary salt-modified clay (Maryam et al. 2013).

Titanium dioxide (TiO_2) is widely used in applications such as photocatalysts, optical coatings, and solar cells (Diebold 2002). The intended end-use depends upon TiO_2 structure. Three types of structures, namely anatase, brookite, and rutile, are available. While anatase and rutile are structurally tetragonal, brookite is orthorhombic (Nam et al. 2012). TiO_2 nanoparticles ($nTiO_2$) have both high specific surface area and fraction of surface atoms. The unique physicochemical features of these particles such as dielectric, optical, and photo catalytic properties have resulted in their use in various applications such as removal of bacteria and harmful organic materials from air and water (Ahmad et al. 2013). Verdier et al. have examined the antibacterial performance of TiO_2 photocatalyst on *E. coli* bacteria (Verdier et al. 2014). Antibacterial effects of different concentrations of TiO_2 were evaluated by Haghi et al. (2012). In view of the above researches, this work aims to examine the antibacterial effectiveness of melt electro-spun polypropylene nano-fibers containing TiO_2 nanoparticles and clay.

Experimental test

Materials

Isotactic polypropylene chips, clay particles, and nano-TiO_2 particles were used in this research. Polypropylene chips and TiO_2 nanoparticles were obtained from Jam Petroleum and Merck Company, respectively. Table 1 shows the characteristics of these materials.

Methods

Polypropylene nano-fibers containing nano-TiO_2 and clay particles were produced in laboratory-scale conventional melt electro-spun apparatus. Despite the vast amount of research on melt electro-spinning of fibers in the past decades, considerable efforts are needed to establish an effective experimental set-up. So far, molten polymer together with needle electro-spinning and rotary metal disk spinnerets have been used to produce polypropylene nano-fibers in previous investigations (Fang et al. 2012). Using these experiences and trial-and-error technique, optimized fiber production adjustments were made. In order to ensure

Table 1 Material characteristics

Polypropylene chips		Clay particles (Tonsil CO 616)		TiO_2 nanoparticles	
Properties (unit)	Value	Properties (unit)	Value	Component	Value (%)
MFI @230 C. 216 kg (g/10 min)	25	Bulk density, Kg/m^3	720	Ceramic, calculated on dried substance	≥99.0
Flexural modulus (Mpa)	1500	Relatively catalyst activity, ton feed/m^3	720	Substance soluble in water	≤0.5
Tensile strength @ yield (Mpa)	32	Loaded volume, m^3	100	Substance soluble in diluted hydrochloric acid	≤0.5
Elongation @ yield (%)	13	Catalyst life time, months	4	Sulfate (So_4)	≤0.05
Vicat softening point, 10 N (°C)	152	Catalyst consumption, batches per year	3	Arsenic (AS)	≤0.005
HDT (0.46 N/mm^2) (°C)	94	Catalyst consumption, tones per year	288	Iron (Fe)	≤0.005

uniform melt, heating system was set well above the melting point of PP. High voltage was set at 20 kV. Spinning distances of 130 and 70 mm were found to be well suited for spinning of nPP/nTiO_2 and nPP/Clay, respectively.

Morphological and FTIR analysis

High-quality SEM and AFM photographs were obtained from webs of nPP/nTiO_2. Hitachi S-4160 and Dual Scope Ds 95-200-E were, respectively, used to obtain the images. Filtration efficiency of the samples is dependent on the factors such as fiber diameter, filter porosity, and fiber distribution. These factors can be determined by image processing technique on the SEM photographs. Thus image processing technique using Matlab software R2009a was employed to estimate percentage average of dominant diameter, porosity, and fiber diameter distribution. Dominant fiber diameter is regarded as the diameter of the majority of the fibers. Microstructure measurement software 3.0 was also used to estimate the average diameter of fiber in the samples. Fourier transform infra-red spectroscopy (FTIR) was used to detect possible chemical changes occurred in polypropylene structure due to addition of nTiO_2 or clay particles. The spectrum recording was achieved using (FTIR: BOMEN MB100), in the range of 400–4000 cm^{-1} and a resolution of 4 cm^{-1}.

Air permeability and dust aerosol analysis

The air permeability of each sample was measured five times using (SDL MO-215) in accordance to BS 5636–1990 test method. Air permeability in mL/s per cm^2 was calculated using Eq. (1):

$$\text{Air permeability} = \frac{q_v}{A}, \tag{1}$$

where q_v and A are the arithmetic mean flow rate of air in mL/s and surface area of the test sample in cm^2, respectively.

Dust aerosol test based on ISO 12103-1 was carried out. Each sample was tested at an air velocity of 0.2 m s^{-1} for 1 h. Upon completion of the test, diameter and surface area of trapped particles were used as indices of dust aerosol.

Antibacterial analysis

Antibacterial ability of each nPP/nTiO_2 and nPP/Clay sample was evaluated 3 times according to 1993–100 AATCC standard test method. LB broth and *E. coli DH5α* as specified in Table 2 were selected as media and bacteria, respectively. Circular 5-cm samples were sterilized in an autoclave for 15 min at 120 °C. Antibacterial performance of the samples as % reduction in number of bacteria based on Eq. (2) was determined.

Table 2 Characteristics of LB broth media and *E. coli DH5α* bacteria

LB broth media properties	
Casein peptone (per liter)	10.00
Yeast extract (per liter)	5.00
Sodium chloride (per liter)	10.00
E.coli DH5α bacteria properties	
Shape	Tube(s)
Product size	2 mL
Competent cell type	Chemically competent
Cloning unstable DNA	Not suitable for cloning unstable DNA
Improved plasmid quality	Yes
Propagating ccdB vectors	Not for ccdB vector propagation
Bacterial or yeast strain	DH5α^{TM}
Transformation efficiency	$>1 \times 10^6$
High-throughput compatibility	Not high-throughput compatible
Regulatory statement	For research use only. Not for any animal or human therapeutic or diagnostic use

$$\text{Reduction rate of bacteria } (\%) = \frac{A - B}{A} \times 100, \quad (2)$$

where A and B denote the number of colonies in controlled microbial dispersion and the number of colonies in the dispersion after co-located adjacent treatment, respectively (Maryam et al. 2013; Periolatto et al. 2014).

Results and discussion

Webs of nano-fibers of polypropylene containing nano-TiO_2 and clay particles were fabricated via purposely designed laboratory-scale melt electro-spun apparatus. Using experiences of the previous researchers together with trial-and-error technique, the most appropriate production adjustments for melt-spinning of the nano-fibers were made. Morphological parameters, such as dominant diameter, average diameter, distribution of nano-fibers, and porosity of the webs, were determined using SEM photographs and image processing technique.

Figures 1 and 2 show the stages used in determination of nano-fiber diameter distribution of nPP/$nTiO_2$ and nPP/Clay during images processing of SEM photographs. A pixel value of 50 nm or 0.05 μ was used throughout.

Morphological characteristics of nPP/Clay and nPP/$nTiO_2$ are summarized in Table 3. The measured fiber diameter and porosity were found to provide the highest filtration efficiency. Dominant fiber diameter or diameter of 88.3 % of the nPP/Clay was found to be 200 nm. The corresponding value of dominant fiber diameter for nPP/$nTiO_2$ was found to be 250 nm of 99.9 % of the fibers. The measured average diameters of both types of fibers were less than the measured dominant diameter. The measured diameters were almost in line with the values of diameter measured by microstructure measurement software. Porosity of nPP/Clay samples was significantly less than that of nPP/$nTiO_2$ samples. The porosity of the samples is in line with their measured diameters. The porosity and pore sizes in the electro-spun nano-fiber webs are basically dependent on the fiber diameter (Soliman et al. 2011). Sample with smaller nano-fiber diameters has lower porosity due to fewer voids within the structure of the web. The use of nano-fibers in comparison to conventional fibers in filtration operation is preferred. This is due to smaller diameter of nano-fibers which results in reduction of porosity of the sample. Significant distribution of fiber diameter can be attributed to conditions under which fibers were produced.

Figure 3 illustrates AFM photographs of nPP/Clay and nPP/$nTiO_2$ samples. The photographs confirm the results provided by the SEM photographs due to

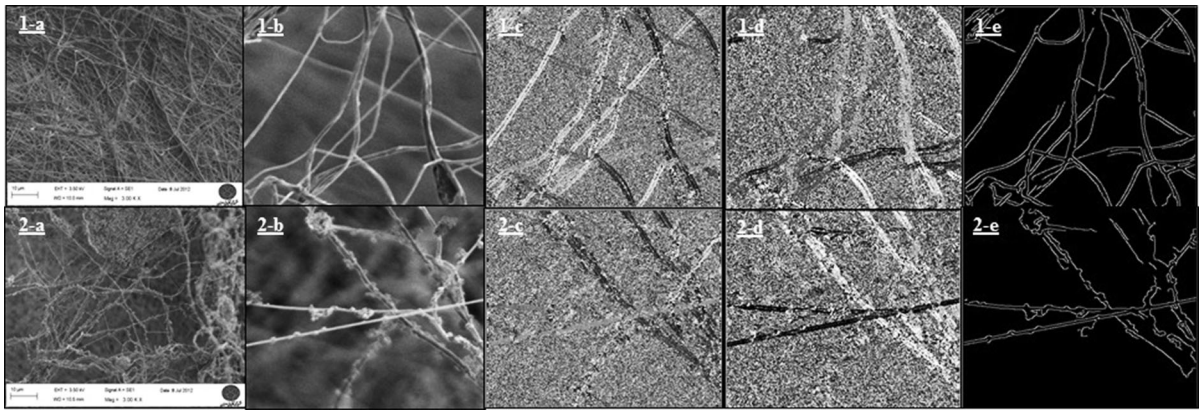

Fig. 1 **a** SEM images of samples, **b** cut image of original SEM as input image, **c** cut image in all angles and orientation, **d** cut image in major 8-angle, **e** edge detector with white color in major angles (the first row = nPP/Clay and the second row = nPP/nTiO$_2$)

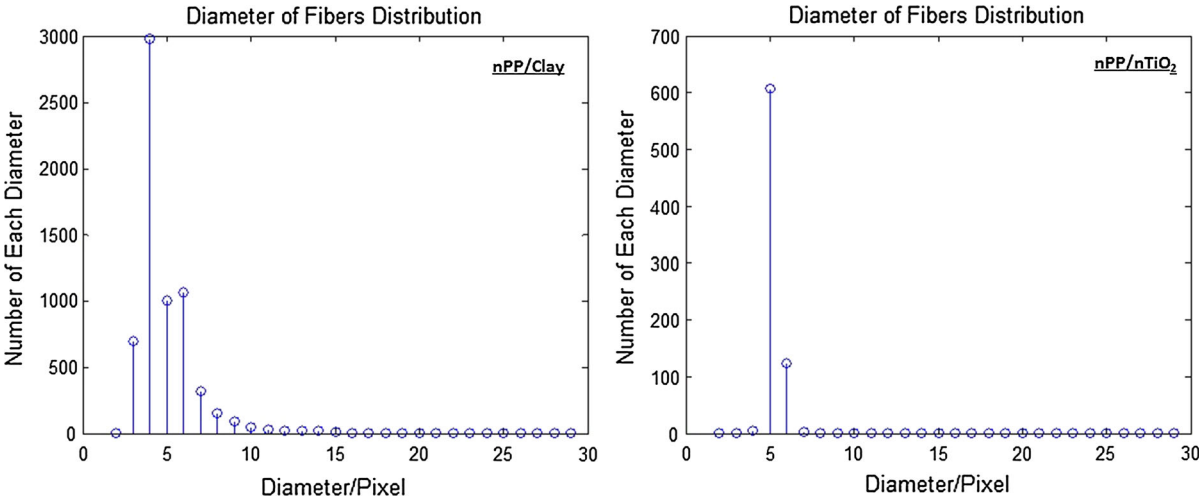

Fig. 2 Nano-fibers' diameter distribution of nPP/Clay and nPP/nTiO$_2$

Table 3 Morphological characteristics of nPP/Clay and nPP/nTiO$_2$ based on image processing and microscopic investigations

Parameters	Image processing method		Microstructure measurement	
	nPP/Clay	nPP/nTiO$_2$	nPP/Clay	nPP/nTiO$_2$
Dominant diameter (nm)	200	250	–	–
Fibers at dominant diameter (%)	88.3	99.9	–	–
Average diameter (nm)	249.3	258.5	242	310
Porosity (%)	60.3	74.1	–	–

diameter distribution of the nano-fibers. Surface distribution in both sets of photographs follows the same trend.

FTIR analysis points to the fact that no chemical changes have occurred in polypropylene melt due to addition of clay or titanium dioxide nanoparticles. In this work, crystallization-sensitive band of 852 cm^{-1} which is within the range of 841–997 cm^{-1}, as reported by previous researches (Reddy et al. 2009; Law et al. 2008), was determined.

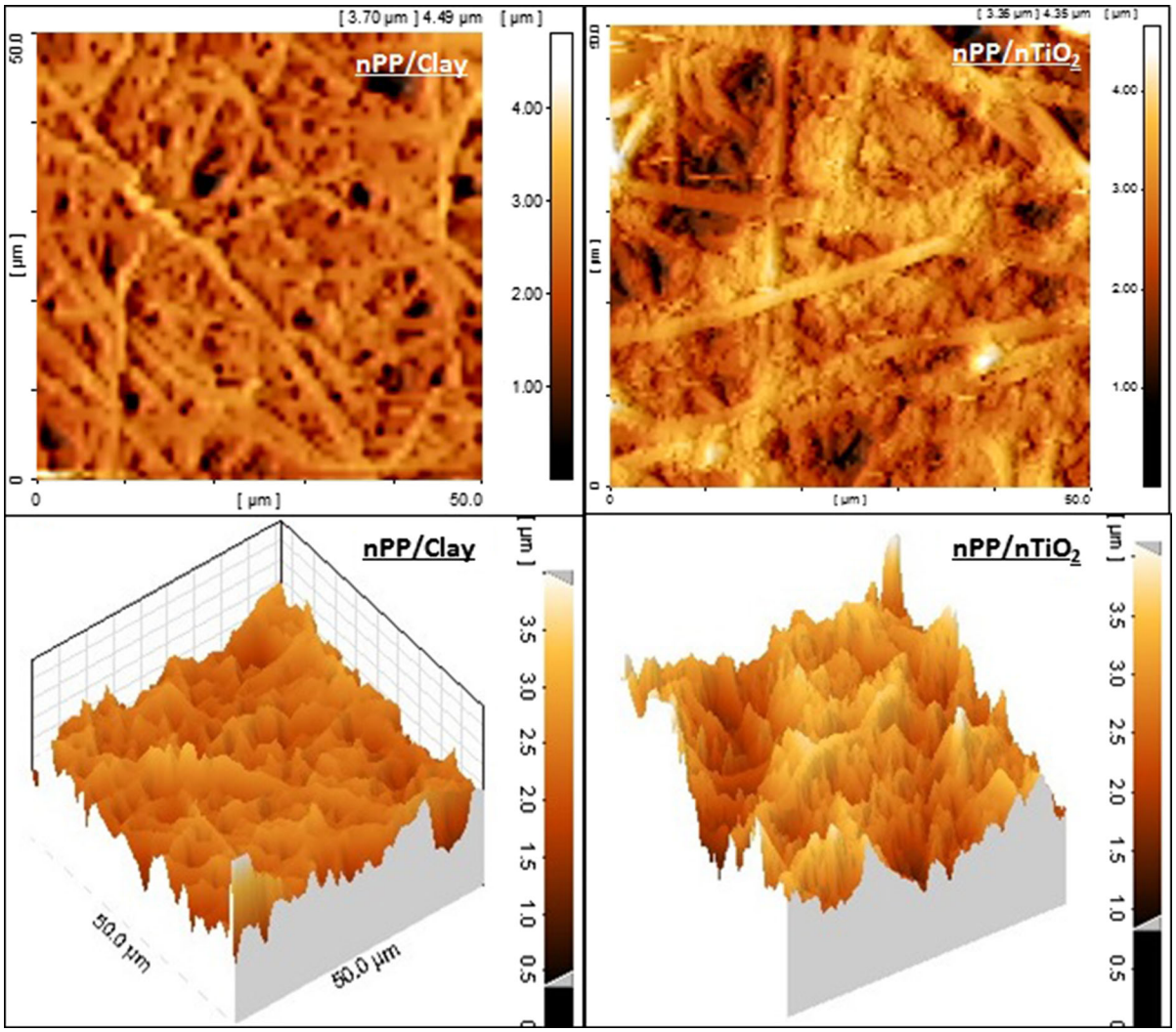

Fig. 3 AFM photographs of nPP/Clay and nPP/$nTiO_2$ samples

FTIR was also used to clarify the dispersion of clay and $nTiO_2$ in PP matrix. Figures 4 and 5 show the FTIR spectra of the nPP/Clay and nPP/$nTiO_2$, respectively. These spectra have an absorption band at 1250 cm^{-1} which is related to C–H bending vibration of PP (Wang et al. 2015). Peaks at 650 cm^{-1} for nPP/$nTiO_2$ and 800 and 450 cm^{-1} for Ti–O stretching bands were observed (Ba-Abbad et al. 2012). The appeared peak in the region of 1726 cm^{-1} is attributed to the absorption of a carbonyl (C=O) group (Kamrannejad et al. 2014). It can be seen that Si–O stretching vibration of clay appears at 1097 cm^{-1} (Innocenzi et al. 2003; Wang et al. 2015) and also the peak at 3367 cm^{-1} is related to the stretching vibration of O–H–O.

Air permeability of the samples due to the importance of the water penetration as a factor of paramount importance is dependent on air permeability. Thus air permeability of the samples as shown in Table 4 was investigated. Results point to the general reduction in air permeability due to addition of either nano-TiO_2 or clay nanoparticles to the polymer melt. The reduction in air permeability of nPP/Clay sample is greater than that of nPP/$nTiO_2$ sample. Air permeability and porosity are of paramount importance in filtration operations. Structural properties are highly influenced

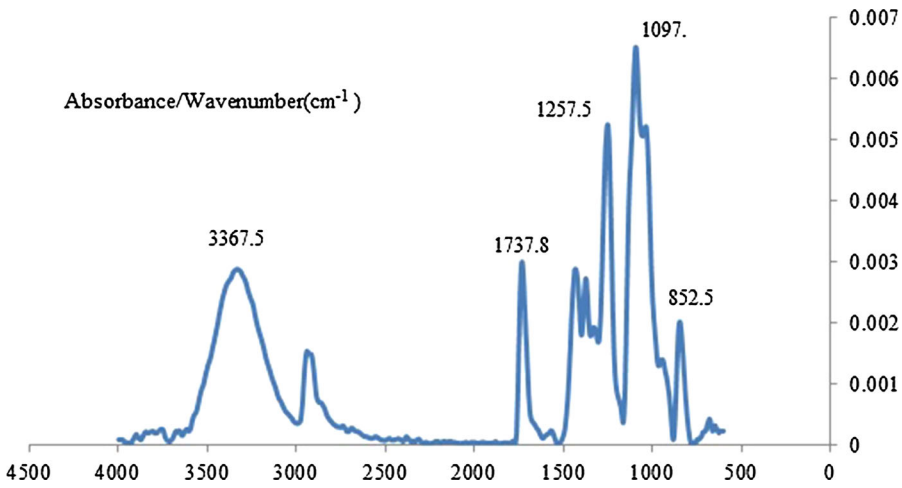

Fig. 4 FTIR spectra of nPP/Clay samples

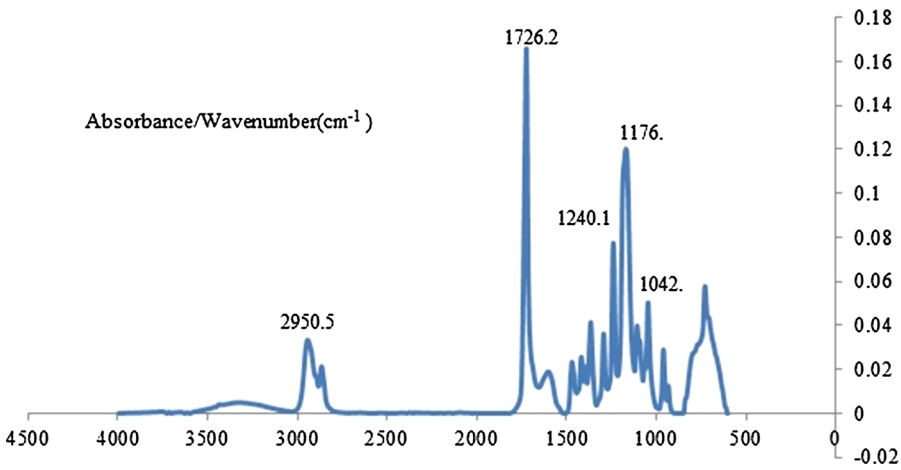

Fig. 5 FTIR spectra of nPP/$nTiO_2$ samples

Table 4 Air and dust permeabilities of samples and antibacterial activity of *E. coli* bacteria

Samples	Air permeability ($mL/s/cm^2$)	Trapped particle diameter (μm)	Trapped particle surface area (μm)	Bacterial reduction rate (%)
PP nano-fibers	10.5	13.2	565.2	–
nPP/$nTiO_2$	9.7	7.4	141.2	69.4
nPP/Clay	9.1	5.2	95.6	88.1

by air permeability which in turn affects sample porosity. The results of dust aerosol tests are in line with reported significant correlation between air permeability and porosity in previous works (Berkalp 2006). Diameter and surface area of the trapped particles of nano-fiber sample containing clay are significantly less than those containing $nTiO_2$ or webs of pure nano-fiber samples. Therefore, it can be said that the addition of nano-TiO_2 or clay particles to the polymer melt leads to spinning of fibers with smaller diameter. This in turn leads to lower porosity and air permeability and subsequent entrapment of smaller particles.

Bacterial activity of *E. coli* bacteria on nPP/Clay and nPP/$nTiO_2$ is shown in Table 4. Bacterial reduction in scales of 88.1 and 69.4 % were obtained for

nPP/nTiO_2 and nPP/Clay, respectively. Results confirm the relative effectiveness of nPP/Clay fibers in comparison to those containing nano-TiO_2 in the elimination of *E. coli* bacteria colonies. Considering the smaller dominant diameter of nano-fibers, the lower porosity, lower air permeability, and the entrapment of particles with smaller diameter and surface area, it can be stated that the nPP/Clay fibers are the most advantageous filter media for filtration of bacteria.

Conclusion

This investigation was aimed to evaluate the relative effectiveness of nano polypropylene filter media containing nano-TiO_2 and clay particles during filtration of bacteria. Factors such as fiber diameter and distribution in the filter media and porosity were measured. Image processing technique was used to estimate fiber dominant diameter and porosity of the prepared media. Suitability of the filter media was confirmed by measurement of air permeability together with diameter and surface area of the entrapped dust aerosols. Additionally, antibacterial efficiency of the samples was examined using *E. coli* bacteria. Results showed that filter media containing nPP/Clay fibers trapped smaller dust aerosols. This was attributed to lower air permeability and porosity of these samples. It was also found that the use of nPP/Clay fibers in comparison to nPP/nTiO_2 fibers is advantageous as far as bacteria reduction is concerned. Finally, it was concluded that due to their unique properties, nano-web samples constitute an effective means of pathogenic microorganism or entrapment of nanoparticles in wet filtration field.

References

Ahmad R, Sardar M (2013) TiO_2 nanoparticles as an antibacterial agents against *E. coli*. Int J Innov Res Sci Eng Technol 2:8

Akinci A (2009) Mechanical and structural properties of polypropylene composites filled with graphite flakes. Arch of Mater Sci Eng 35:91

Ba-Abbad MM et al (2012) Synthesis and catalytic activity of TiO_2 nanoparticles for photochemical oxidation of concentrated chlorophenols under direct solar radiation. Int J Electrochem Sci 7:4871

Berkalp OB (2006) Air permeability and porosity in spun-laced fabrics. Fibres Text East Eur 14:57

Bhorodwaj SK, Dutta DK (2011) Activated clay supported heteropoly acid catalysts for esterification of acetic acid with butanol. Appl Clay Sci 53:347

Diebold U (2002) Structure and properties of TiO_2 surfaces: a brief review. Appl Phys A 76:1

Fang J, Zhang L, Sutton D, Wang X, Lin T (2012) Needleless melt-electrospinning of polypropylene nanofibres. J Nanomater 9: ID 382639

Gao Y, Truong YB, Zhu Y, Kyratzis IL (2014) Electrospun antibacterial nano-fibers: production, activity, and in vivo applications. J Appl Polym Sci. doi:10.1002/APP.40797

Ghiasi M, Naghashzargar E, Semnani D (2014) Silk fibroin nano-coated textured silk yarn by electrospinning method for tendon and ligament scaffold application. Nano Hybrids 7:35

Gitipour S, Baghvand A, Givehchi S (2006) Adsorption and permeability of contaminated clay soils to hydrocarbons. Pak J Biol Sci 9:336

Haghi M et al (2012) Antibacterial effect of TiO_2 nanoparticles on pathogenic strain of *E. coli*. Int J Adv Biotechnol Res 3:621

Housmans JW, Gahleitner M, Peters GWM, Meijer HEH (2009) Structure–property relations in molded, nucleated isotactic polypropylene. Polymer 50:2304

Innocenzi P (2003) Infrared spectroscopy of sol–gel derived silica-based films: a spectra-microstructure overview. J Non-Cryst Solids 316:309

Kamrannejad MM, Hasanzadeh A (2014) Photocatalytic degradation of polypropylene/TiO_2 nano-composites. Mater Res. doi:10.1590/1516-1439.267214

Law A, Simon L, Sullivan P (2008) Effect of thermal aging on isotactic polypropylene crystallinity. Poly Eng Sci 48:627

Lyons J, Li C, Ko F (2004) Melt-electrospinning part I: processing parameters and geometric properties. Polymer 45:7597

Maryam AS, Montazer M, Rashidi A, Rahimi MK (2013) Antibacterial properties of clay layers silicate: a special study of montmorillonite on cotton fiber. Asian J Chem 25:2889

Mirjalili M, Yaghmaei N, Mirjalili M (2013) Antibacterial properties of nano silver finish cellulose fabric. J Nanostruct Chem 3:43

Nam SH, Cho SJ, Boo JH (2012) Growth behavior of titanium dioxide thin films at different precursor temperatures. Nanoscale Res Lett 7:89

Nayak PS, Singh BK (2007) Instrumental characterization of clay by XRF, XRD and FTIR. Bull Master Sci 30:235

Parolo ME (2011) Antibacterial activity of materials synthesized from clay minerals. In: Mendez-Vilas A (ed) Science against microbial pathogens: communicating current research and technological advances, vol 144. Formatex Research Center, Badajoz

Periolatto M, Ferrero F, Vineis C, Varesano A (2014) Antibacterial water filtration by cationized or chitosan coated cotton gauze. Chem Eng Trans 38:235

Phong NTP, Thanh NVK, Phuong PH (2009) Fabrication of antibacterial water filter by coating silver nanoparticles on flexible polyurethane foams. J Phys Confer Ser 187:012079

Polanco C (2013) Selective antibacterial peptides: a review on their polarity. In: Mendez-Vilas A (ed) Microbial

pathogens and strategies for combating them: science, technology and education. Formatex Research Center, Badajoz, p 1307

Reddy KR et al (2009) Structural evolution process of isotactic polypropylene in the isothermal crystallization from the melt. J Phys 184:012001

Soliman S et al (2011) Controlling the porosity of fibrous scaffolds by modulating the fiber diameter and packing density. J Biomed Mater Res A 96A:566

Uddin F (2008) Clays, nanoclays, and montmorillonite minerals. Metall Mater Trans A 39(12):2804–2814

Verdier T, Coutand M, Bertron A, Roques C (2014) Antibacterial activity of TiO_2 photocatalyst alone or in coatings on *E. coli*: the influence of methodological aspects. Coatings 4:670

Wang L, He A (2015) Microstructure and thermal properties of polypropylene/clay nanocomposites with $TiCl_4/MgCl_2$/-clay compound catalyst. J Nanomater. doi:10.1155/2015/591038

Zhong C, Mao B (2014) Single ethylene molecular insertion as a probe into the nature of the active species in MgCl2-supported Ziegler–Natta catalysts. J Mol Catal A 395:283